

SA-106 Grade B Pipe Fracture Dataset

Michael Kozluk¹

¹ P.Eng., Consultant, Burlington, Ontario, CANADA (MikeKozluk@yahoo.ca)

Abstract

Scott et al. (1992) presented version 1 of a database of pipe fracture experiments compiled by two of the leading research institutes that had conducted pipe fracture testing, Battelle in the United States of America (USA) and MPA in Germany. The database compiled pipe fracture tests that had been performed since the late 1950s. In the early years, researchers focused their attention on studying the failure pressure and crack propagation behaviour of axially cracked pipes loaded by internal pressure. The earliest work was sponsored by the oil and gas industry and involved relatively thin-walled, low-toughness carbon steel pipes. This work was eventually followed up by efforts in the USA and Germany on nuclear piping with axial cracks. Subsequently, attention turned to understanding the behaviour of circumferentially cracked nuclear piping subjected to both pressure and bending loads. The loading histories for these experiments ranged from the relatively simple case of quasi-static, monotonic displacement control, to the more complex cases of dynamic cyclic loading and pipe system experiments. The database included data for straight pipes with circumferential flaws (cracks) from Battelle, MPA, and other organizations.

Version 1 of the pipe fracture database for circumferential cracks was expanded and version 2.2b of the database was released, Scott and Wilkowski (1996). Version 3 of the database was released as a deliverable from the International Piping Integrity Research Group (IPIRG) programs.

Fields were added and entries were modified based on verification against the cited documentation by the current author. From this modified pipe fracture database, a dataset of 105 pipe fracture tests SA106 Grade B pipes with circumferential cracks were extracted. This material is of particular interest because it is used for the large-diameter piping in the main circuit of CANDU[®] nuclear power plants. This paper documents the SA-106 Grade B pipe fracture dataset and uses it to show that the net-section collapse flow model is a good engineering model for predicting the maximum load-carrying capacity of pressurized sections of SA-106 Grade B pipe containing circumferential flaws.

1 INTRODUCTION

Since the 1950s, researchers worldwide have conducted thousands of pipe fracture experiments. The results from these pipe fracture experiments greatly improved the understanding of the behaviour of straight pipes and piping components containing crack-like flaws under overload conditions. For example, the evidence indicates that the “instantaneous” double-ended guillotine break could not happen in large-diameter nuclear-grade piping under normal operation or accident loading conditions. For the pipe to fail it is necessary to postulate the existence of a very large flaw and a loading event several times larger than the design-basis earthquake. In the 1980s, the results of these pipe fracture experiments were used to establish the technical basis for methods to resolve some of the outstanding licensing issues associated with the design methodologies for the dynamic effects associated with the postulated rupture of primary coolant piping. This led to the leak-before-break (LBB) methodology used in the United States and the break preclusion methodology used in Germany and France. These methodologies were used to justify the elimination of the requirement for pipe whip restraints for pressurized water reactors. With the evolution of regulatory positions on the application of LBB and the high costs associated with testing large-diameter pipes, the impetus for pipe fracture testing decreased and relatively little testing (of large-diameter) pipes was conducted after the mid-1990s.

1.1 IPIRG pipe fracture database

Scott et al. (1992) presented version 1 of a database of pipe fracture experiments compiled by two of the leading research institutes that had conducted pipe fracture testing, Battelle in the USA and MPA in Germany. The pipe fracture database for circumferential cracks was expanded and version 2.2b of the database was released, Scott and Wilkowski (1996). Version 3 of the database was released as a deliverable from the International Piping Integrity Research Group (IPIRG) programs. In this paper, version 3 of the database is referred to as the IPIRG circumferential-crack pipe fracture database or simply the IPIRG pipe fracture database.

The IPIRG pipe fracture database was released as a Lotus 123 spreadsheet. Figure 1 provides a breakdown of the types and numbers of experiments in the database that includes 860 records (pipe fracture experiments). Individual experiments (database records) were grouped according to the cited source of the data. Table 1 lists the 38 fields that make up the individual records in the IPIRG pipe fracture database.

2 DATABASE MODIFICATIONS

The IPIRG pipe fracture database was converted from a Lotus 123 spreadsheet to an Excel workbook. This section describes the modifications made by the author to the IPIRG pipe fracture database.

2.1 Added fields

Six fields were added to each record in the database.

- Test ID This is a unique, consecutive integer number that is used to reference individual database records/experiments. There are 860 records/experiments and the Test ID ranges from 1 to 860.
- Material ID This is an integer number assigned to the pipe material. Table 2 lists the assigned Material ID.
- Flaw ID This is an integer in the range 1 to 5 that designates the type of crack/ flaw as illustrated in Figure 2. When the flaw geometry is not specified, the flaw type is assumed to be either no crack, inside surface crack, or through-wall crack. The type of flaw assumed is based on the value of the specified flaw depth. Note that in the case of the complex crack (Flaw ID = 5), the wall thickness used for the net-section collapse calculation is the ligament thickness ($t - a$).
- Load ID This is an integer that designates the type of loading applied.
- 1 Monotonic bending, either three-point or four-point bending. Includes quasi-static and dynamic loading rates.
 - 2 Monotonic tension, internal pressure and/or axial tensile force.
 - 3 Cyclic bending, either three-point or four-point bending.
 - 4 Cyclic tension, internal pressure and/or axial tensile force.
 - 5 Inertial loading is typically performed as four-point bending.
 - 6 IPIRG piping system tests.
- ASME Yield Table Y-1 of ASME (1995) gives the yield strength (S_y) values for Section III materials as a function of the metal temperature. Quadratic expressions were used to curve-fit the yield strength values for SA-106 Grades A and B and SA-312 Grades TP304 and TP316L over the range of 100°F to 700°F. These expressions were used to provide the ASME/BPVC specified yield strength at the test temperature for records of these four materials.

ASME Ultimate Table U of ASME (1995) gives the ultimate tensile strength (S_u) values for Section III materials as a function of the metal temperature. Quadratic expressions were used to curve-fit the ultimate tensile strength values for SA-106 Grades A and B and SA-312 Grades TP304 and TP316L over the range of 100°F to 700°F. These expressions were used to provide the ASME/BPVC specified ultimate tensile strength at the test temperature for records of these four materials.

2.2 Changes

In addition to adding the columns and headings for the six new fields described above, this section describes changes that were made to the database records. Some of these changes were made to facilitate programming that was ultimately used to extract various datasets from the database.

2.2.1 Formatting

The following editorial changes were made:

- Delete blank columns and some of the blank rows.
- Introduce some row/column rules (borders) and page breaks.
- Modify the title block and collect all generic notes there.

2.2.2 Notes and comments

Remove “flags” from the test quantities (P_{max} , M_i , M_{max}). The note flags were appended to the experiment ID instead. The following test records were modified: 3, 53, 58, 313, 365, 366, 372, 373, 403-408, 416, 417, 428, 455-462, 471-483, 484-489, 455-462, 556, 557, 582, 583, 589-592, 598, 724-727, 847-852.

For test record 833, remove note flags append to experiment ID and set Flaw ID = 0 as it is not a valid test because no flaw length or depth was given.

NUREG references in the “QA review performed by” column were cleared and the references were appended to the “Comment” column for the following test records: 54-57, 365-373.

2.2.3 ASME material properties

As described in Section 2.1, values for S_y and S_u were provided for the following.

Material ID = 111	SA-106 Grade A, for records: 228-230, 234, 235, 377, 505.
Material ID = 112	SA-106 Grade B, for records: 6, 25, 54-57, 72-80, 92-95, 114-164, 236, 237, 313-315, 342, 343, 365, 367, 369, 371, 398, 401, 406-410, 432-448, 596-598, 603, 710-719, 772, 774, 775, 838, 840, 844, 845, 851-853.
Material ID = 310	SA-312 Grade TP304, for records: 15, 17, 23, 32, 34, 36, 39, 42, 45, 47-49, 53, 65-71, 81-91, 96-100, 184-190, 211-215, 219, 220, 267, 268, 310, 311, 316, 317, 340, 350-363, 366, 368, 370, 399, 400, 403-405, 413-418, 455-463, 582-584, 586-592, 600, 606, 682-689, 724-733, 767-771, 773, 776-782, 790, 792-795, 800-803, 808-811, 813, 821-826, 830-835, 839, 841, 843, 846-848, 854-860.
Material ID = 331	SA-312 Grade TP316L, for records: 7, 8, 26-31, 60, 101-105, 170-177, 231-233, 238-260, 374-376, 402, 420-429, 449-452, 506, 602.

2.2.4 Tensile tests

Changed M_{max} from “NA” to “0”, P set equal to P_{max} (psi), and set P_{max} to “0” for the following tensile test records: 340-345, 705-719, 350-363, 724-736.

2.2.5 Elbow Tests

Modify test records 605 and 845 so that the pipe geometry and material properties are used instead of the elbow properties.

2.2.6 Calculation of M_{max}

M_{max} is defined as $(L_o-L_i) \times P_{max}/4$ for the following test records: 286-297 and 578-581.

The kinematic correction was removed and M_{max} was defined as $(L_o-L_i) \times P_{max}/4$. This was done because the author could not reproduce the correction factor (and it is a second-order complication). This was done to the following test records with (old/new) values indicated:

3 (40993.0/42273.9),	53 (342.3/374.0),	58 (744.2/744.3),	365 (426.5/436.0),
366 (306.2/334.0),	403 (261.2/270.9),	404 (527.3/557.6),	405 (892.8/993.2),
406 (336.2/343.8),	407 (708.6/727.4),	408 (1039.0/1074.6),	416 (533.4/575.2),
417 (561.8/713.2),	428 (136.0/1179.5),	429 (392.3/386.2),	589 (825.0/948.3),
590 (560.0/557.0),	591 (474.7/542.1),	592 (8776.0/9353.1),	847 (242.4/251.1),
848 (160.4/163.8),	849 (231.5/238.5),	850 (172.3/175.5),	851 (293.7/297.9),
852 (177.5/179.1)			

2.2.7 Verification changes

Copies of most of the references cited in the IPIRG pipe fracture database were obtained and used to verify as many entries in the database as possible. Checked entries in columns A-Z, but did not change initiations values (P_i , M_i) if they were the only discrepancy. The initialism "OHN" was appended to the entry in the "QA review performed by" column.

- Eiber et al. (1971) was used to check test records 715-719. The value of t was changed to agree with the "average" thickness from Table 6 of reference, and the a/t was changed accordingly.
- Data record book entries were provided by Battelle to IPIRG members. These were used to check test records: 54-57, 72, 313-315, 365, 367, 369, 371, 398, 401, 406-410, 596-598, 603, 605, 772, 774, 775, 838, 840, 844, 851-853. Modifications were made to the following test records:

72: Temperature changed from "125" to "137" and the yield & ultimate values changed from "41.1" & "71.7" to "38.4" & "71.3".

401: t changed from "1.030" to "1.039" and M_{max} changed from "7,541" to "7,540".

605: P_i , P_{max} , M_i , M_{max} changed from "48.50, 54.50, 6114, 6861" to "50.09, 56.02, 6312, 7059" and yield stress in the elbow & pipe changed from "31.3 & 30.0" to "31.4 & 30.4".

838: crack length changed from "43.8" to "52.5" and M_{max} changed from "3020" to "2970".

840: crack length & depth changed from "48 & 69.1" to "42 & 69".

845: elbow wall thickness changed from "1.32" to "1.37", M_{max} was missing and made "7213", yield in the elbow & pipe changed from "31.3 & 30.0" to "31.4 & 30.4".

- Milella (1987 and 1998) were used to check carbon steel pipe test records 6, 114-164, 432-448. Some modifications were made to M_{max} , but they were very minor (last decimal place) and were probably due to inconsistent values used for unit conversion. The M_{max} for test record 6 was missing.
- Vassilaros et. al. (1984) was used to check test records 72-80. Table 2 of reference was used: modified outside diameter to agree with R and t values and the crack lengths were determined using R (mean radius) and specified crack lengths.
- Milella (1987 and 1998) were used to check stainless steel pipe test records 7, 8, 165-183, 449-454. No M_{max} available to check tests 7, 8, 453, 454. Some modifications were made to M_{max} , but they were very minor (last decimal place) and were probably due to inconsistent values used for unit conversion.
- The following test records were not checked because cited references were not available: 92-95, 342, 343, 710-714.
- The following test records were not checked because cited references did not contain sufficient information: 25, 228-230, 234-237, 377, 505.

3 NET-SECTION COLLAPSE FLAW MODEL

The net-section collapse (NSC) flaw model was used as a regression model for the SA-106 Grade B pipe fracture dataset. The underlying limit load assumption is that the pipe is made of a rigid perfectly plastic material. The model is for a single constant depth rectilinear circumferential crack that is centred on the location of maximum tensile bending stress as illustrated in Figure 3.

The limitations of the NSC model are:

- The piping material must be sufficiently ductile that failure is governed by the strength of the material and not the fracture toughness.
- The pipe contains a single rectilinear, constant depth flaw centred at the location of maximum bending stress in the section of the pipe.

The expressions for surface circumferential flaws in a straight pipe have been generalized to address that the flaw can be connected to the outside surface, or it can be embedded, or it can be connected to the inside surface.

Figure 4 illustrates the three different flaw geometries that are considered with this flaw model.

- Short flaws are contained in the tensile region of the pipe cross-section.
- Long flaws without crack-face closure, the flaw extends into the compressive region of the pipe cross-section. This geometry is appropriate for long flaws that have sufficient width so that the faces in the compressive region do not come into contact.
- Long flaws with crack-face closure, the flaw extends through the entire tensile region of the pipe cross-section. This geometry is appropriate for long, tight flaws such as arise from fatigue and stress corrosion cracking.

Figure 5 is a flowchart illustrating how the net-section collapse flow model is used to calculate the maximum bending moment that can be carried by a section of straight pipe containing a circumferential flaw. The dimensionless parameter λ depends on the mean diameter of the pipe, D , the nominal wall thickness of the pipe, t , and the type of flaw, α .

$$\lambda = 2\alpha(1 + \alpha) \frac{t/D}{(1 - t/D)^2} \quad (1)$$

where $\alpha = \begin{cases} -1 & \dots \text{for an outside surface flaw} \\ 0 & \dots \text{for an internal (embedded) flaw} \\ +1 & \dots \text{for an inside surface flaw} \end{cases}$

The reference force, F_o , is the axial force corresponding to the limit load of the unflawed pipe subjected to pure tension, (i.e., zero pressure and no bending moment). The reference internal pressure, P_o , is the internal pressure corresponding to the limit pressure (considering the axial direction) of the unflawed pipe subjected to pure pressure, (i.e., zero axial load and no bending moment). The reference bending moment, M_o , is the bending moment corresponding to the limit load of the unflawed pipe subjected to pure bending, (i.e., zero pressure and no axial force). These parameters are a function of the mean diameter, D , nominal wall thickness, t , and the flow strength, σ_f .

$$\begin{aligned} F_o &= \pi D t \sigma_f \\ P_o &= \frac{4(t/D)}{(1 - t/D)^2} \sigma_f \\ M_o &= D^2 t \sigma_f \end{aligned} \quad (2)$$

The effect of internal pressure acting on the faces of an inside surface flaw is accounted for by scaling the internal pressure.

$$P^* = \left\{ 1 + \lambda \frac{\theta a}{\pi t} \left[1 - \frac{t}{D} \left(1 - \frac{a}{t} \right) \right] \right\} P \quad (3)$$

3.1 Short flaws

In the case of flaws that do not extend into the region of the cross-section below the neutral axis, (i.e., $2\theta \leq 2\pi - 2\beta$), the bending moment corresponding to the state of net-section collapse is:

$$M_{NSC} = M_o \left\{ \sin \beta - \frac{1}{2} \left[1 - \left(1 + \alpha \frac{a t}{t D} \right)^2 \left(1 - \frac{a}{t} \right) \right] \sin \theta \right\} \quad (4)$$

where the location of the neutral axis is:

$$\beta = \frac{\pi}{2} \left\{ 1 - \frac{\theta a}{\pi t} \left[1 - \alpha \frac{t}{D} \left(1 - \frac{a}{t} \right) \right] - \left(\frac{P^*}{P_o} + \frac{F}{F_o} \right) \right\} \quad (5)$$

3.2 Long flaws

In the case of flaws that extend into the region of the cross-section below the neutral axis, (i.e., $2\theta > 2\pi - 2\beta$), there are two possibilities.

3.2.1 Without crack-face closure

If the faces of the flaw in the compressive region of the cross-section do not touch, then the bending moment corresponding to the state of net-section collapse is:

$$M_{NSC} = M_o \left\{ \left(1 + \alpha \frac{a}{t} \frac{t}{D} \right)^2 \left(1 - \frac{a}{t} \right) \sin \beta + \frac{1}{2} \left[1 - \left(1 + \alpha \frac{a}{t} \frac{t}{D} \right)^2 \left(1 - \frac{a}{t} \right) \right] \sin \theta \right\} \quad (6)$$

where the location of the neutral axis is:

$$\beta = \frac{\frac{\pi}{2} \left\{ 1 - \left(2 - \frac{\theta}{\pi} \right) \frac{a}{t} \left[1 - \alpha \frac{t}{D} \left(1 - \frac{a}{t} \right) \right] - \left(\frac{P^*}{P_o} + \frac{F}{F_o} \right) \right\}}{1 - \frac{a}{t} \left[1 - \alpha \frac{t}{D} \left(1 - \frac{a}{t} \right) \right]} \quad (7)$$

3.2.2 With crack-face closure

If the faces of the flaw in the compressive region of the cross-section touch, then the bending moment corresponding to the state of net-section collapse is:

$$M_{NSC} = \frac{M_o}{2} \left\{ 1 + \left(1 + \alpha \frac{a}{t} \frac{t}{D} \right)^2 \left(1 - \frac{a}{t} \right) \right\} \sin \beta \quad (8)$$

where the location of the neutral axis is:

$$\beta = \frac{\pi \left\{ 1 - \frac{a}{t} \left[1 - \alpha \frac{t}{D} \left(1 - \frac{a}{t} \right) \right] \left(1 + \lambda \frac{P}{P_o} \right) - \left(\frac{P}{P_o} + \frac{F}{F_o} \right) \right\}}{2 - \frac{a}{t} \left[1 - \alpha \frac{t}{D} \left(1 - \frac{a}{t} \right) \right] \left(1 + \lambda \frac{P}{P_o} \right)} \quad (9)$$

4 SA-106 GRADE B PIPE FRACTURE DATASET

Visual basic for applications procedures and functions were added to the Excel workbook to automate the extraction, reduction, and presentation of the tests from the modified pipe fracture database. Table 3 lists the 105 monotonic bending tests of SA-106 Grade B pipes. The five different flaw types (Flaw ID) are illustrated in Figure 2. The measured (failure) bending moment is taken as the maximum value of the bending moment measured in the test. For carbon steel pipe tests, the maximum bending moment can be significantly greater in value than the bending moment at which the extension of the circumferential flaw initiates. Two of the tests were excluded as statistical outliers, leaving 103 tests in the SA-106 Grade B pipe fracture dataset. The first test excluded was 126, which had the maximum variance and was an obvious erroneous data point attributed to a transcription error. To “balance” this test 603, the test with the minimum variance, was also excluded.

The dataset includes defects primarily in parent material (a limited number of pipes had defects in circumferential girth butt welds) and loading was monotonic and applied either as a quasi-static or dynamic load application. That is tests that involved cyclic loading (see Figure 1) were excluded because of the

complication of fatigue crack growth before stable/unstable crack growth. Figure 6 summarizes the range of test parameters for the 103 monotonic bending tests in the SA-106 Grade B pipe fracture dataset.

- The majority (73 of 103) of the tests were conducted on through-wall flaws.
- The size of the test pipes ranges from NPS 2 to NPS 16, with the majority (43 of 103) of the tests being conducted on NPS 6 pipes.
- The tests were conducted at one of three test temperatures: ambient temperature, 130°F, and 560°F. The majority (58 of 103) of the tests were conducted at ambient temperature.
- The tests were conducted with one of three internal pressure values: zero, 1.6 ksi, or 2.25 ksi. The majority (97 of 103) of the tests were not pressurized.

5 VALIDATION OF THE NSC FLAW MODEL

The NSC flaw model was used to predict the maximum bending moment (M_{NSC}) for all of the tests, which are included in Table 3. To reduce the experimental data, the long flaw formulation with crack-face closure was used together with the following definition for the flow strength:

$$\sigma_f = 1.30 \left(\frac{S_y + S_u}{2} \right) \quad (10)$$

where S_y and S_u are the values of the yield strength and ultimate tensile strength specified in Section II of the ASME/BPVC.

Table 4 summarizes the general statistics of the regression of the maximum bending moments from the tests against the bending moment predicted by the NSC flaw model. The value of the predicted NSC bending moment M_{NSC} is proportional to the assumed value of the flow strength so the comparison of the measured maximum bending moment and the predicted NSC bending moment is dependent upon the value of the flow strength used. Figure 7 includes a plot of the test against predicted data. In that plot, the three diagonal lines correspond to “measured equals predicted” for three different definitions of the flow strength. The flow strength is defined by the value of the flow strength factor (FSF), which is the scaling factor applied to the average of the ASME/BPVC specified yield and ultimate tensile strengths for SA-106 Grade B pipe at the test temperature.

$$\sigma_f = FSF \left(\frac{S_y + S_u}{2} \right) \quad (11)$$

- A flow strength equated to 1.30 times the average of the ASME/BPVC specified yield and ultimate tensile strengths ($FSF = 1.30$ line) corresponds to the “best fit” of the regression analysis. The maximum bending moment measured in 52 of the 103 tests (50%) is conservatively predicted. The r^2 statistic for the simple regression of M_{test}/M_o onto M_{NSC}/M_o is 0.9864, which indicates that the NSC flaw model explains 98.64% of the variability in M_{test}/M_o and from this, it is concluded that the NSC model does an excellent job of predicting the maximum load-carrying capacity of this dataset of monotonic bending tests of SA-106 Grade B pipes with circumferential flaws.
- If the flow strength is equated to 1.141 times the average of the ASME/BPVC specified yield and ultimate tensile strengths ($FSF = 1.141$ line), then this corresponds to the 90% lower-bound model. The maximum bending moment measured in 93 of the 103 tests (90%) is conservatively predicted by the NSC flaw model.

- If the flow strength is equated to 1.10 times the average of the ASME/BPVC specified yield and ultimate tensile strengths ($FSF = 1.10$ line), then the maximum bending moment in 100 of the 103 tests (97%) is conservatively predicted by the NSC flaw model.

Figure 7 includes a plot of the cumulative distribution of the standardized variance from regression; where variance is defined as one minus the predicted value divided by the measured value. This plot illustrates that the variance between the measure and predicted maximum bending moments can be assumed to be normally distributed.

5.1 Applicability

The range of applicability for the NSC flaw model is based on the SA-106 Grade B pipe fracture dataset that was used to validate the flaw model.

- The circumferential extent of the through-wall circumferential cracks is less than one-half of the circumference of the pipe.
- The ratio of the mean radius to the wall thickness of the pipe (R/t) is in the range of 5 to 20.

5.2 Summary

This validation demonstrates that the NSC flaw model is a good engineering model for predicting the maximum load-carrying capacity of pressurized sections of SA-106 Grade B pipe containing circumferential cracks.

6 CLOSING

A dataset of 103 pipe fracture tests of monotonic bending of SA-106 Grade B pipes with circumferential flaws has been extracted from the IPIRG pipe fracture dataset. This dataset was used to validate the net-section collapse flaw model for constant-depth, circumferential flaws in straight sections of pressurized carbon-steel pipes.

7 NOMENCLATURE

7.1 List of acronyms

ASME	American Society of Mechanical Engineers
BMI	Battelle Memorial Institute
BPVC	Boiler and Pressure Vessel Code, ASME
CANDU	CANada Deuterium natural Uranium reactor CANDU is a registered trademark of Atomic Energy of Canada Limited.
ENEA	Nuclear Energy and Alternative Energies, Italy
ID	identifier
IPIRG	International Piping Integrity Research Group
LBB	leak-before-break
MPA	Staatliche Materialprüfungsanstalt University of Stuttgart, Germany
NPS	nominal pipe size
NRC	U.S. Nuclear Regulatory Commission
NSC	net-section collapse
NUREG	U.S. Nuclear Regulatory Commission Report
NUREG/CR	U.S. Nuclear Regulatory Commission Contractor Report
PFDB	pipe fracture database
PVP	pipng and pressure vessels
OHN	Ontario Hydro, Nuclear
QA	quality assurance

7.2 List of symbols

a	geometry	the depth of the surface flaw.
A_i	geometry	the inside area of the pipe.
D	geometry	the mean diameter of the pipe.
D_o	geometry	the outside diameter of the pipe.
F	NSC flaw model	axial force.
F_o	NSC flaw model	reference axial force. The limit load axial force of an unflawed pipe for pure tension, (i.e., no internal pressure and no bending moment).
FSF	NSC flaw model	flow-strength factor.
L_i	geometry	the inner span of the 4-point bend loading fixture.
L_o	geometry	the outer span of the 4-point bend loading fixture.
M	NSC flaw model	bending moment at the cross-section of the pipe containing the circumferential flaw. A positive value (sense) produces a maximum tensile axial (bending) stress at the centre of the circumferential flaw.

M_i	PFDB	bending moment corresponding to crack initiation.
M_{max}	PFDB	maximum bending moment measured in a test.
M_{NSC}	NSC flaw model	bending moment corresponding to a state of net-section collapse of a straight section of pressurized pipe containing a circumferential flaw.
M_o	NSC flaw model	reference bending moment. The limit load bending moment for an unflawed pipe for pure bending, i.e., zero internal pressure and no axial force.
M_{pred}	NSC flaw model	predicted maximum bending moment.
M_{test}	PFDB	maximum bending moment measured in a pipe fracture test.
P	NSC flaw model	internal pressure.
	PFDB	applied load for bend test and internal pressure for burst test.
P^*	NSC flaw model	internal pressure scaled to account for crack-face pressure.
P_i	PFDB	applied load for bend test and internal pressure for burst test corresponding to crack initiation.
P_{max}	PFDB	maximum applied load for bend test and internal pressure for burst test.
P_o	NSC flaw model	reference pressure. The limit load pressure in the axial direction of the unflawed pipe for pressure only, (i.e., no axial force or bending moment).
R	geometry	the mean radius of the pipe.
r^2	statistics	coefficient of determination
s	statistics	standard deviation.
S_u	material properties	ASME/BPVC Section III, Class 1 specified tensile strength.
S_y	material properties	ASME/BPVC Section III, Class 1 specified yield strength.
t	geometry	the nominal wall thickness of the pipe.
α	NSC flaw model	dimensionless multiplier indicating the location of the flaw $-1/0/+1$ for flaws on the outside/middle/inside surfaces, respectively.
β	NSC flaw model	the angular location of the neutral axis in the cross-section of the pipe containing the flaw.
λ	NSC flaw model	a dimensionless term that is a function of the type of flaw and the thickness-to-diameter ratio of the pipe.
μ	statistics	mean value.
π	constant	the ratio of the circumference of a circle to its diameter, $\pi = 3.14159\dots$
2θ	NSC flaw model	the total extent/length of the circumferential crack.
σ_f	material properties	flow strength.

8 REFERENCES

- ASME (1995). ASME Boiler & Pressure Vessel Code, Section II: Materials Part D – Properties, 1995 July 1.
- Eiber, R.J., Maxey, W.A., Duffy, A.R., Atterbury, T.J. (1971). *Investigation of the Initiation and Extent of Ductile Pipe Rupture – Final Report*, Battelle Memorial Institute Report BMI-1908.
- Milella, P.P. (1987), *Outline of Nuclear Piping Research Conducted in Italy*, Nuclear Engineering and Design, Volume 98, pp. 219–229.
- Milella, P.P. (1998). FAX to Keith Wichman (NRC), *Summary of ENEA/DISP Pipe Fracture Experiments*.
- Scott, P., Wilkowski, G., Sturm, D., Stoppler, W. (1994). *Development and a Database of Pipe Fracture Experiments*, Nuclear Engineering and Design, Volume 151, pages 359-371.
- Scott, P.M., Wilkowski, G.M. (1996). *Development and Application of a Database of Pipe Fracture Experiments*, Fatigue and Fracture, Volume 1, PVP Volume 323, pages 13-26.
- Vassilaros, M.G., Hays, R.A., Gudas, J.P., Joyce, J.A. (1984). *J-Integral Tearing Instability Analyses for 8-Inch Diameter ASTM A106 Steel Pipe*, U.S. Nuclear Regulatory Commission Report NUREG/CR-3740, 1984 April.

Table 1: IPIRG Pipe Fracture Database Fields

This table lists the 38 fields that make up the individual records of the IPIRG pipe fracture database.

Field Type	Field Description
Test Parameters	Data record book number (Battelle experiments only).
	Experiment identifier.
	Pipe identifier (Battelle experiments only).
	Material.
	Outer diameter (inches).
	Schedule of pipe.
	Pipe wall thickness (inches).
	Test temperature (°F).
	Inner span (inches).
	Outer span (inches).
	Internal pressure (psi).
	Length of the crack (expressed as a percentage of the pipe circumference).
	Depth of the crack (expressed as a percentage of the wall thickness).
	Applied load at crack initiation (kips).
	Maximum applied load (kips).
Bending moment at crack initiation (kip·in).	
Maximum bending moment (kip·in).	
Number of loading cycles (for cyclic tests).	
Tensile Properties	Yield stress from axial tension tests (ksi).
	Ultimate stress from axial tension tests (ksi).
	Percentage elongation from axial tensile tests (%).
	Area reduction from axial tensile tests (%).
	Reference stress for a Ramberg-Osgood characterization (ksi).
	Reference strain for a Ramberg-Osgood characterization.
	Coefficient for a Ramberg-Osgood characterization.
	Exponent for a Ramberg-Osgood characterization.
Material ID used for Ramberg-Osgood characterization (Battelle experiments only).	
Fracture Properties	The J-integral for initiation (lbf/in).
	The change in J-integral with crack extension (lbf/in ²).
	The J-integral for initiation for a power-law characterization (lbf/in).
	The coefficient for a power-law characterization.
	The exponent for a power-law characterization
	Material ID used for power-law characterization (Battelle experiments only).
Impact Properties	The upper shelf impact energy (lbf·in).
	The room temperature impact energy (lbf·in).
	The room temperature percentage shear area.
Quality Assurance	Summary of quality assurance reviews.
Comment	Field for test-specific comments.

Table 2: Material Identifiers for Modified PFDB

Mat. ID	Family	IPIRG PFDB Designation	Comment
100	carbon steel	CS	carbon steel from Germany or Japan
100	carbon steel	A53 GrB(a)	carbon steel for galvanized pipes
100	carbon steel	A710	age-hardening low-carbon NiCuCrMoNb, NiCuNb, and NiCuMgNb alloy
100	carbon steel	AISI 1020	SAE carbon steel
100	carbon steel	ANSI1020 ERW seam	? SAE carbon steel
100	carbon steel	StE 460	high strength low-alloy steel (DIN 17102); similar to A633(E) (centrifugally cast carbon steel for high temperature services)
111	carbon steel	A106A	carbon steel for high-temperature services
112	carbon steel	A106B	carbon steel for high-temperature services
115	carbon steel	A106B Elbow	carbon steel for high-temperature services
120	carbon steel	A155KC60CL1	electric-fusion welded pipe steel for high pressure services; replaced by A671, A672, and A673 (1978); made from A515 Gr.60 plate
134	carbon steel	A516 Gr 70	carbon steel for pressure vessel plates; (moderate- and low-temperature services)
140	carbon steel	SA333 Gr6	carbon and alloy pipe steel for low-temperature services
150	carbon steel	St. 20 CS	German carbon steel
150	other	NiMoCr-Melt	other steel
150	other	11NiMnCrMo55	other steel
150	other	15NiCuMoNb5	other steel
150	other	MnMoNiV-Melt	other steel
150	other	17MnMoV64	other steel
150	other	20MnMoNi55	German steel
150	other	15Mo3	other steel
161	carbon steel	STS42	Japanese carbon steel
162	carbon steel	STS-49	Japanese carbon steel
163	carbon steel	STS410	Japanese carbon steel from Hitachi
172	carbon steel	API-5LX60	API alloy steel
173	carbon steel	API-5LX65	API alloy steel
174	carbon steel	API-5LX70	API alloy steel
300	stainless steel	SS	stainless steel
300	stainless steel	10GN2MFA SS	? Russian stainless steel; ? carbon steel, SMIRT-12, Aug 93, p429-434
310	stainless steel	TP304	stainless steel
310	stainless steel	w/SA-240 TP304L	stainless steel
320	stainless steel	TP308 Weld	stainless steel
321	stainless steel	TP308L Weld	stainless steel
330	stainless steel	TP316	stainless steel
331	stainless steel	TP316L	stainless steel
332	stainless steel	TP316LN	stainless steel
333	stainless steel	TP316L-S	stainless steel
334	stainless steel	TP316L-mod	stainless steel
335	stainless steel	Z3CND17-12	French stainless steel; equivalent to TP316L
341	stainless steel	Unaged CF8M	stainless steel; cast
342	stainless steel	Aged CF8M	stainless steel; cast
350	other	10 CrNiTi 18 9	other steel; looks like X10CrNiNb 18 9, Nb-stabilized ss
350	other	10CrMoNiNb910	other steel
350	other	X20CrMoV12 1	other steel
350	other	X10CrNiNb18 9	other steel; Nb-stabilized ss
350	other	XCrNiNb18 9	other steel
350	stainless steel	1.4541 SS	German stainless steel
350	stainless steel	No.1.4948(a)	German stainless steel; cast
410	other	Inconel 600	other
410	other	Inconel	other
420	other	F316 SafeEnd	bi-metallic
420	other	Bimetal Weld	other

Table 3: SA-106 Grade B Pipe Fracture Dataset

This table lists the IPIRG pipe fracture database of 105 monotonic bending tests for SA-106 Grade B pipes. The five different flaw types (Flaw ID) are illustrated in Figure B-1. The two outliers, Test ID 603 and 126, are highlighted with shading and strike-through font and are excluded as statistical outliers. The tests are sorted first by flaw type and then by test number.

Test ID	Flaw ID	D_o (in)	t (in)	θ/π (-)	a/t (-)	Temp. (°F)	P (ksi)	F (kip)	M_{test} (kip·in)	α (-)	σ_f (ksi)	M_o (kip·in)	M_{nsc} (kip·in)	M_{test}/M_{NSC} (-)	M_{test}/M_o (-)	M_{NSC}/M_o (-)	variance (-)
6	1	6.625	0.720	0	0	68	0	0	1,396	0	61.22	1,537	1,537	0.908	0.908	1.000	-0.101
25	1	6.625	0.433	0	0	572	0	0	1,031	0	56.74	942	942	1.095	1.095	1.000	0.086
406	2	6.666	0.293	0.508	0.631	550	0	0	344	1	56.95	678	390	0.882	0.507	0.575	-0.134
407	2	6.594	0.582	0.503	0.680	550	0	0	727	1	56.95	1,198	658	1.105	0.607	0.549	0.095
408	2	6.621	0.845	0.526	0.633	550	0	0	1,075	1	56.95	1,605	963	1.116	0.669	0.600	0.104
409	2	15.850	1.040	0.532	0.662	550	0	0	6,623	1	56.95	12,991	7,071	0.937	0.510	0.544	-0.068
410	2	15.940	0.500	0.535	0.662	550	0	0	3,235	1	56.95	6,788	3,602	0.898	0.477	0.531	-0.114
596	2	15.874	0.999	0.500	0.670	550	2.25	0	5,260	1	56.95	12,588	5,307	0.991	0.418	0.422	-0.009
597	2	6.595	0.531	0.432	0.647	550	2.25	0	683	1	56.95	1,112	595	1.149	0.614	0.535	0.129
598	2	6.589	0.552	0.419	0.720	550	2.25	0	545	1	56.95	1,146	554	0.983	0.476	0.484	-0.017
603	2	24.000	1.680	0.250	0.605	550	2.25	0	22,794	±	56.95	47,664	34,026	0.670	0.478	0.714	-0.493
432	3	4.500	0.437	1.000	0.350	68	0	0	357	-1	61.22	442	331	1.078	0.808	0.749	0.073
433	3	4.500	0.437	1.000	0.500	68	0	0	272	-1	61.22	442	271	1.004	0.615	0.613	0.004
434	3	4.500	0.437	1.000	0.700	68	0	0	170	-1	61.22	442	175	0.974	0.386	0.396	-0.027
435	3	4.500	0.437	1.000	0.700	68	0	0	170	-1	61.22	442	175	0.974	0.386	0.396	-0.027
436	3	4.500	0.437	1.000	0.250	68	0	0	322	-1	61.22	442	366	0.879	0.729	0.830	-0.138
437	3	4.500	0.437	1.000	0.500	68	0	0	272	-1	61.22	442	271	1.004	0.615	0.613	0.004
438	3	4.500	0.437	1.000	0.250	68	0	0	272	-1	61.22	442	366	0.741	0.615	0.830	-0.349
439	3	6.626	0.535	1.000	0.500	68	0	0	799	-1	61.22	1,216	753	1.061	0.657	0.619	0.057
440	3	6.626	0.535	1.000	0.500	68	0	0	771	-1	61.22	1,216	753	1.024	0.634	0.619	0.023
441	3	6.626	0.535	1.000	0.250	68	0	0	1,030	-1	61.22	1,216	1,014	1.016	0.847	0.834	0.016
442	3	6.626	0.535	1.000	0.250	68	0	0	1,023	-1	61.22	1,216	1,014	1.009	0.841	0.834	0.009
443	3	6.626	0.744	1.000	0.500	68	0	0	1,022	-1	61.22	1,576	955	1.070	0.649	0.606	0.065
444	3	8.626	0.406	1.000	0.250	68	0	0	1,299	-1	61.22	1,678	1,413	0.919	0.774	0.842	-0.088
445	3	8.626	0.406	1.000	0.500	68	0	0	1,266	-1	61.22	1,678	1,061	1.193	0.754	0.632	0.162
446	3	8.626	0.406	1.000	0.500	68	0	0	1,409	-1	61.22	1,678	1,061	1.328	0.840	0.632	0.247
447	3	8.626	0.406	1.000	0.250	68	0	0	1,297	-1	61.22	1,678	1,413	0.918	0.773	0.842	-0.090
448	3	8.626	0.429	1.000	0.500	68	0	0	1,286	-1	61.22	1,765	1,115	1.154	0.729	0.631	0.133
51	4	6.625	0.435	0.304	1.000	550	0	0	454	-1	56.95	949	456	0.997	0.479	0.480	-0.003
54	4	6.600	0.550	0.360	1.000	550	0	0	454	-1	56.95	1,146	449	1.011	0.396	0.392	0.011
55	4	6.592	0.539	0.372	1.000	550	0	0	366	-1	56.95	1,125	421	0.871	0.326	0.374	-0.148
56	4	6.579	0.516	0.372	1.000	550	0	0	403	-1	56.95	1,080	404	0.997	0.373	0.374	-0.003
57	4	6.591	0.542	0.373	1.000	550	0	0	416	-1	56.95	1,129	421	0.988	0.368	0.372	-0.012
72	4	8.600	0.540	0.328	1.000	137	0	0	833	-1	60.91	2,137	943	0.883	0.390	0.441	-0.133
73	4	8.591	0.551	0.300	1.000	125	0	0	957	-1	61.02	2,173	1,057	0.905	0.440	0.486	-0.105
74	4	8.616	0.536	0.302	1.000	125	0	0	800	-1	61.02	2,135	1,032	0.776	0.375	0.483	-0.289
75	4	8.618	0.538	0.262	1.000	125	0	0	1,058	-1	61.02	2,143	1,179	0.898	0.494	0.550	-0.114
76	4	8.657	0.597	0.248	1.000	125	0	0	1,089	-1	61.02	2,367	1,358	0.802	0.460	0.574	-0.247
77	4	8.606	0.546	0.232	1.000	125	0	0	1,144	-1	61.02	2,164	1,301	0.879	0.528	0.601	-0.138
78	4	8.606	0.526	0.215	1.000	125	0	0	1,192	-1	61.02	2,095	1,322	0.901	0.569	0.631	-0.110
79	4	8.693	0.573	0.192	1.000	125	0	0	1,317	-1	61.02	2,305	1,547	0.851	0.571	0.671	-0.175
80	4	8.620	0.560	0.210	1.000	125	0	0	1,221	-1	61.02	2,220	1,420	0.860	0.550	0.640	-0.163
92	4	8.594	0.537	0.301	1.000	550	0	0	828	-1	56.95	1,985	963	0.860	0.417	0.485	-0.163
93	4	8.605	0.544	0.295	1.000	550	0	0	911	-1	56.95	2,013	996	0.915	0.453	0.495	-0.093
94	4	8.618	0.542	0.330	1.000	550	0	0	749	-1	56.95	2,013	882	0.849	0.372	0.438	-0.178
95	4	8.604	0.536	0.319	1.000	550	0	0	800	-1	56.95	1,987	906	0.883	0.403	0.456	-0.132
114	4	6.626	0.701	0.250	1.000	572	0	0	772	-1	56.74	1,396	796	0.970	0.553	0.570	-0.031
115	4	6.626	0.717	0.417	1.000	572	0	0	428	-1	56.74	1,420	440	0.973	0.302	0.310	-0.028
116	4	6.626	0.720	0.500	1.000	572	0	0	285	-1	56.74	1,426	295	0.967	0.200	0.207	-0.034
117	4	6.626	0.732	0.333	1.000	572	0	0	587	-1	56.74	1,443	626	0.938	0.407	0.434	-0.066

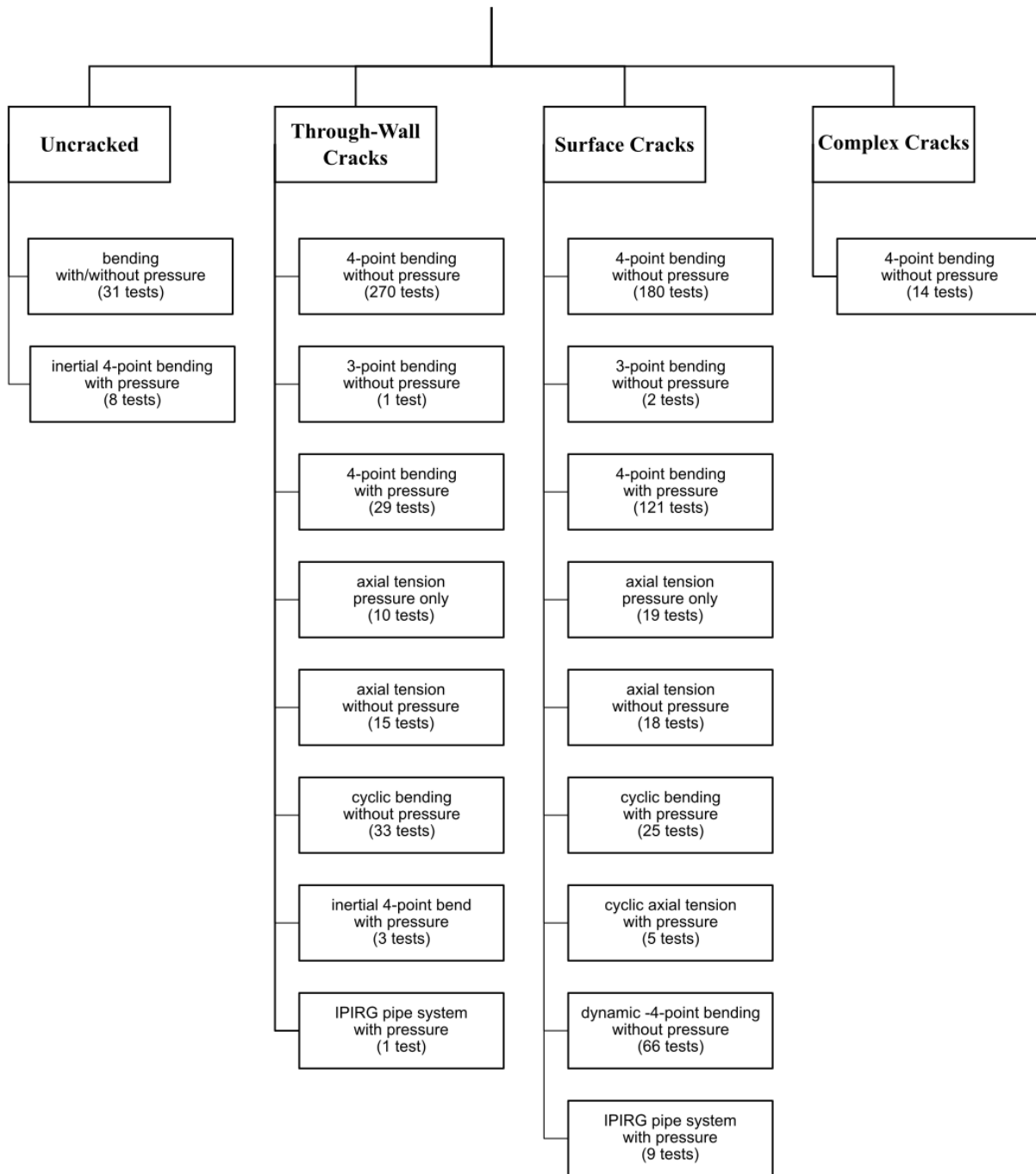
Test ID	Flaw ID	D_o (in)	t (in)	θ/π (-)	a/t (-)	Temp. (°F)	P (ksi)	F (kip)	M_{test} (kip·in)	α (-)	σ (ksi)	M_o (kip·in)	M_{nsc} (kip·in)	M_{test}/M_{NSC} (-)	M_{test}/M_o (-)	M_{NSC}/M_o (-)	variance (-)
118	4	6.626	0.740	0.167	1.000	572	0	0	980	-1	56.74	1,455	1,041	0.941	0.673	0.715	-0.062
119	4	8.626	0.728	0.250	1.000	572	0	0	1,368	-1	56.74	2,578	1,470	0.931	0.531	0.570	-0.075
120	4	8.626	0.732	0.167	1.000	572	0	0	1,777	-1	56.74	2,589	1,852	0.960	0.686	0.715	-0.042
121	4	8.626	0.740	0.500	1.000	572	0	0	535	-1	56.74	2,612	541	0.988	0.205	0.207	-0.012
122	4	8.626	0.752	0.333	1.000	572	0	0	1,018	-1	56.74	2,645	1,147	0.887	0.385	0.434	-0.127
123	4	8.626	0.752	0.417	1.000	572	0	0	767	-1	56.74	2,645	820	0.935	0.290	0.310	-0.069
124	4	2.374	0.217	0.125	1.000	68	0	0	53	-1	61.22	62	49	1.088	0.859	0.789	0.081
125	4	2.374	0.217	0.153	1.000	68	0	0	60	-1	61.22	62	46	1.305	0.966	0.740	0.234
126	4	2.374	0.217	0.153	1.000	68	0	0	102	-1	61.22	62	46	2.229	1.650	0.740	0.551
127	4	2.374	0.217	0.188	1.000	68	0	0	48	-1	61.22	62	42	1.155	0.783	0.678	0.134
128	4	2.374	0.217	0.250	1.000	68	0	0	42	-1	61.22	62	35	1.190	0.678	0.570	0.159
129	4	4.500	0.429	0.250	1.000	68	0	0	236	-1	61.22	435	248	0.952	0.543	0.570	-0.050
130	4	4.500	0.433	0.375	1.000	68	0	0	154	-1	61.22	439	162	0.952	0.352	0.370	-0.050
131	4	4.500	0.437	0.125	1.000	68	0	0	306	-1	61.22	442	349	0.877	0.693	0.789	-0.140
132	4	4.500	0.437	0.524	1.000	68	0	0	84	-1	61.22	442	80	1.046	0.190	0.181	0.044
133	4	4.500	0.673	0.083	1.000	68	0	0	478	-1	61.22	604	521	0.919	0.792	0.863	-0.089
134	4	4.500	0.673	0.167	1.000	68	0	0	438	-1	61.22	604	432	1.014	0.725	0.715	0.013
135	4	4.500	0.673	0.375	1.000	68	0	0	275	-1	61.22	604	223	1.231	0.455	0.370	0.188
136	4	4.500	0.724	0.259	1.000	68	0	0	426	-1	61.22	632	351	1.213	0.673	0.555	0.176
137	4	4.500	0.724	0.267	1.000	68	0	0	412	-1	61.22	632	342	1.205	0.652	0.541	0.170
138	4	4.500	0.724	0.267	1.000	68	0	0	412	-1	61.22	632	342	1.205	0.652	0.541	0.170
139	4	4.500	0.724	0.509	1.000	68	0	0	146	-1	61.22	632	125	1.173	0.231	0.197	0.147
140	4	4.500	0.724	0.515	1.000	68	0	0	150	-1	61.22	632	121	1.245	0.238	0.191	0.197
141	4	4.500	0.724	0.521	1.000	68	0	0	149	-1	61.22	632	117	1.275	0.235	0.184	0.216
142	4	4.500	0.724	0.529	1.000	68	0	0	133	-1	61.22	632	111	1.193	0.210	0.176	0.162
143	4	6.626	0.531	0.500	1.000	68	0	0	283	-1	61.22	1,209	250	1.132	0.235	0.207	0.117
144	4	6.626	0.539	0.375	1.000	68	0	0	471	-1	61.22	1,223	452	1.042	0.385	0.370	0.040
145	4	6.626	0.543	0.125	1.000	68	0	0	989	-1	61.22	1,231	972	1.018	0.804	0.789	0.018
146	4	6.626	0.551	0.250	1.000	68	0	0	694	-1	61.22	1,245	710	0.978	0.558	0.570	-0.023
147	4	6.626	0.720	0.056	1.000	68	0	0	1,339	-1	61.22	1,538	1,398	0.958	0.870	0.909	-0.044
148	4	6.626	0.720	0.389	1.000	68	0	0	584	-1	61.22	1,538	537	1.087	0.379	0.349	0.080
149	4	6.626	0.720	0.667	1.000	68	0	0	135	-1	61.22	1,538	103	1.317	0.088	0.067	0.241
150	4	6.626	0.740	0.125	1.000	68	0	0	1,285	-1	61.22	1,570	1,239	1.037	0.819	0.789	0.036
151	4	6.626	0.740	0.241	1.000	68	0	0	957	-1	61.22	1,570	920	1.040	0.609	0.586	0.039
152	4	6.626	0.740	0.252	1.000	68	0	0	911	-1	61.22	1,570	890	1.023	0.580	0.567	0.023
153	4	6.626	0.740	0.253	1.000	68	0	0	903	-1	61.22	1,570	887	1.017	0.575	0.565	0.017
154	4	6.626	0.740	0.375	1.000	68	0	0	611	-1	61.22	1,570	580	1.052	0.389	0.370	0.050
155	4	6.626	0.740	0.489	1.000	68	0	0	384	-1	61.22	1,570	345	1.116	0.245	0.220	0.104
156	4	6.626	0.740	0.491	1.000	68	0	0	351	-1	61.22	1,570	341	1.030	0.224	0.217	0.029
157	4	6.626	0.740	0.509	1.000	68	0	0	359	-1	61.22	1,570	310	1.160	0.229	0.197	0.138
158	4	8.626	0.406	0.500	1.000	68	0	0	371	-1	61.22	1,678	347	1.068	0.221	0.207	0.064
159	4	8.626	0.417	0.500	1.000	68	0	0	358	-1	61.22	1,722	357	1.004	0.208	0.207	0.004
160	4	8.626	0.417	0.500	1.000	68	0	0	405	-1	61.22	1,722	357	1.135	0.235	0.207	0.119
161	4	8.626	0.425	0.375	1.000	68	0	0	689	-1	61.22	1,751	647	1.065	0.394	0.370	0.061
162	4	8.626	0.429	0.125	1.000	68	0	0	1,255	-1	61.22	1,765	1,393	0.901	0.711	0.789	-0.110
163	4	8.626	0.433	0.250	1.000	68	0	0	895	-1	61.22	1,780	1,015	0.882	0.503	0.570	-0.134
164	4	8.626	0.437	0.375	1.000	68	0	0	582	-1	61.22	1,794	663	0.877	0.324	0.370	-0.140
236	4	6.625	0.433	0.333	1.000	572	0	0	372	-1	56.74	942	408	0.911	0.395	0.434	-0.098
237	4	6.625	0.433	0.083	1.000	572	0	0	760	-1	56.74	942	813	0.935	0.807	0.863	-0.069
313	4	15.905	0.996	0.370	1.000	550	1.60	0	3,907	-1	56.95	12,608	3,651	1.070	0.310	0.290	0.065
314	4	15.720	1.030	0.120	1.000	550	2.25	0	9,185	-1	56.95	12,658	9,426	0.974	0.726	0.745	-0.026
315	4	6.650	0.440	0.249	1.000	550	2.25	0	481	-1	56.95	966	468	1.028	0.497	0.484	0.027
851	5	6.625	0.385	0.370	1.000	550	0	0	298	-1	56.95	853	322	0.926	0.349	0.377	-0.080
852	5	6.625	0.200	0.370	1.000	550	0	0	179	-1	56.95	470	177	1.011	0.381	0.377	0.011
853	5	6.500	0.268	0.384	1.000	550	0	0	227	-1	56.95	593	211	1.074	0.383	0.356	0.069

Table 4: NSC Regression Statistics

This table summarizes the general statistics for the regression of the net-section collapse model using a flow strength of $\sigma_f = 1.30 \times \frac{1}{2}(S_y + S_u)$ for the SA-106 Grade B monotonic bending pipes test dataset.

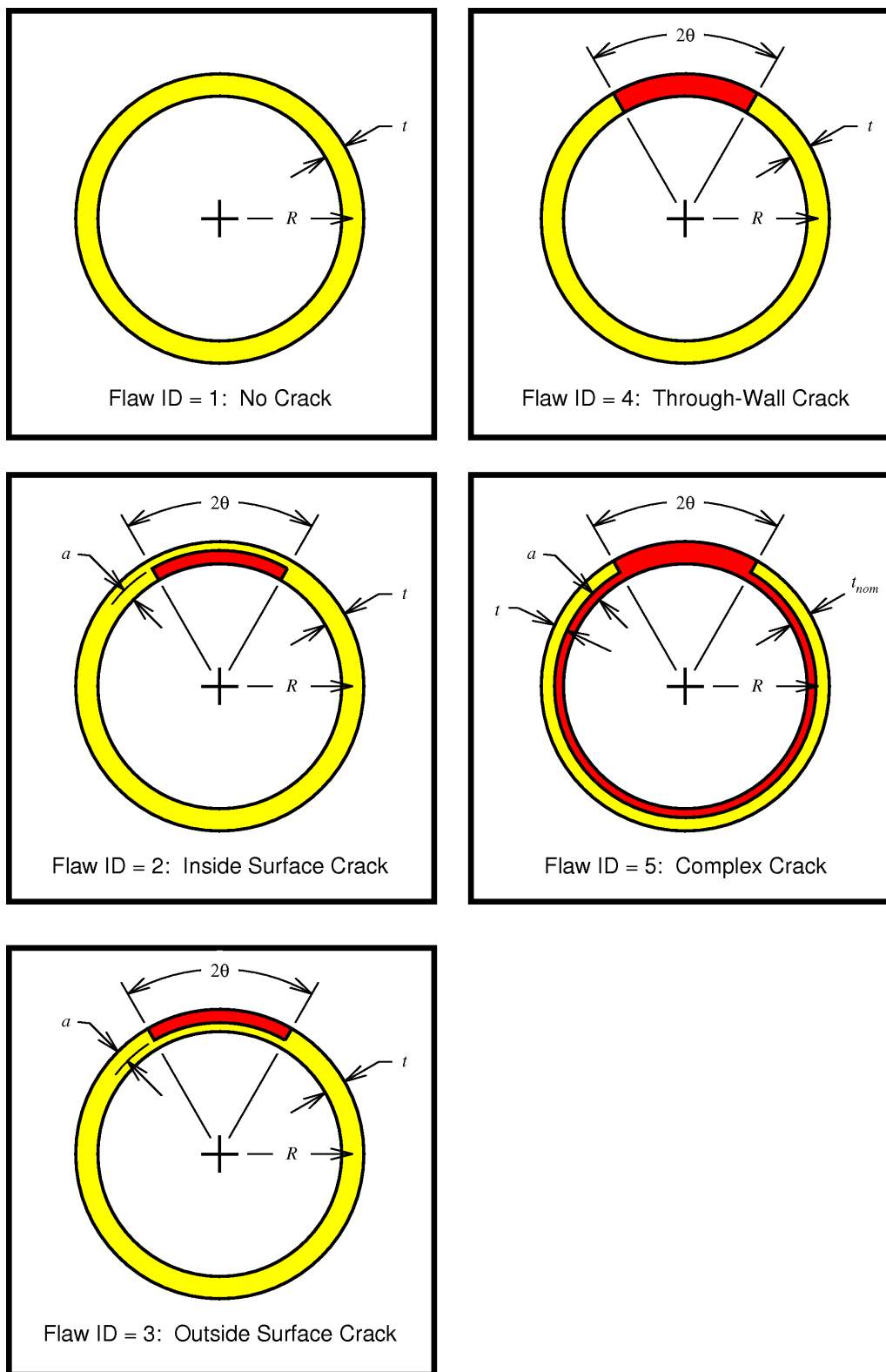
	M_{test}/M_{NSC}	Variance ($1 - M_{NSC}/M_{test}$)
count	103	103
minimum	0.741	-0.349
maximum	1.328	0.247
range	0.587	0.596
mean (μ)	1.011	-0.003
median	0.997	-0.003
standard deviation (s)	0.122	0.117
coefficient of skewness	0.547	-0.074
coefficient of kurtosis	-0.015	-0.022
count > (μ)	46 (45%)	52 (50%)
count > ($\mu-1s$)	18 (17%)	19 (18%)
count > ($\mu-2s$)	4 (4%)	3 (3%)

IPIRG Pipe Fracture Database



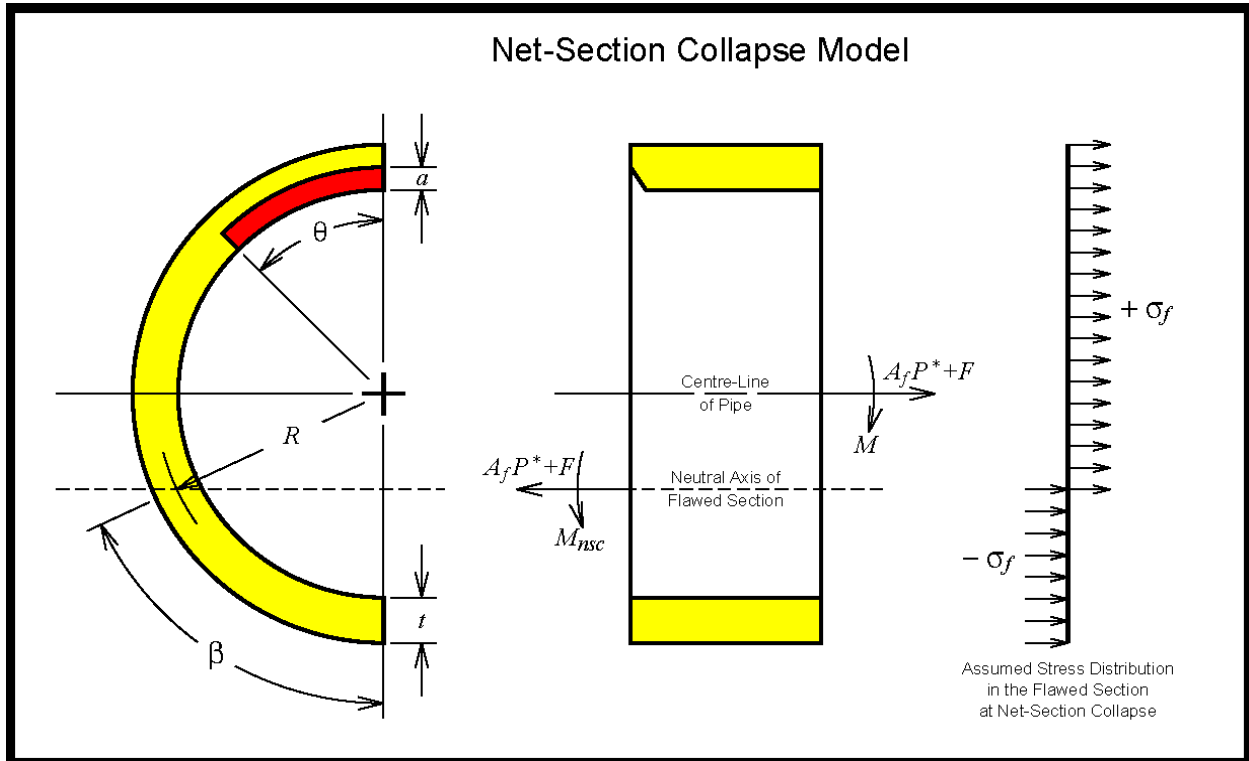
This chart provides a breakdown of the different types and numbers of tests in the IPIRG pipe fracture database.

Figure 1: Contents of IPIRG Pipe Fracture Database



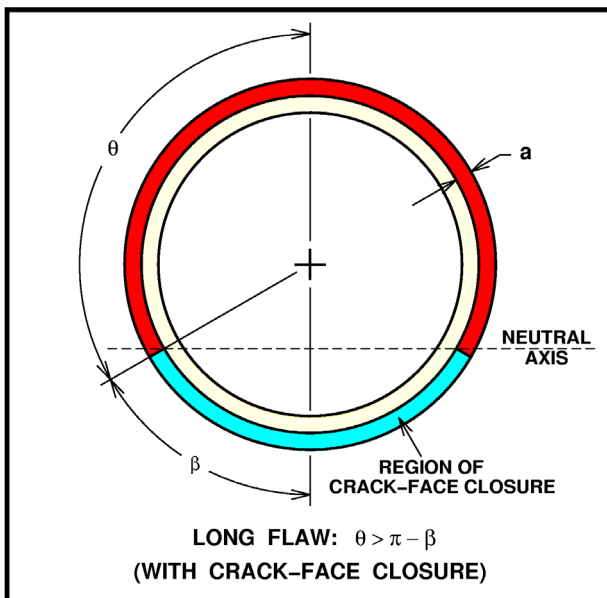
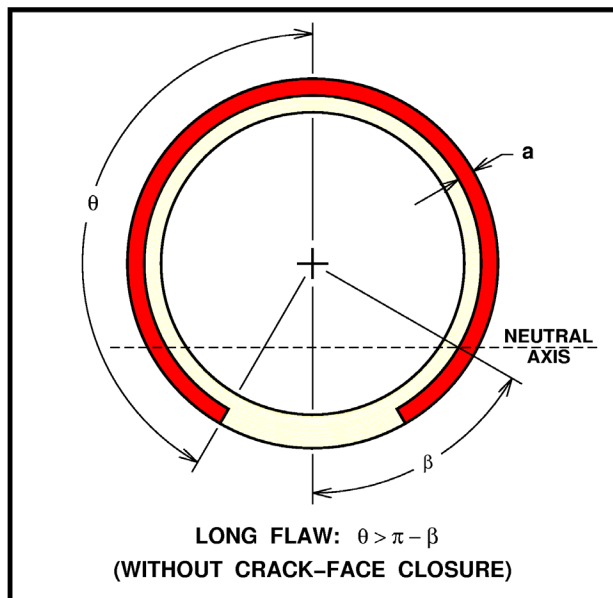
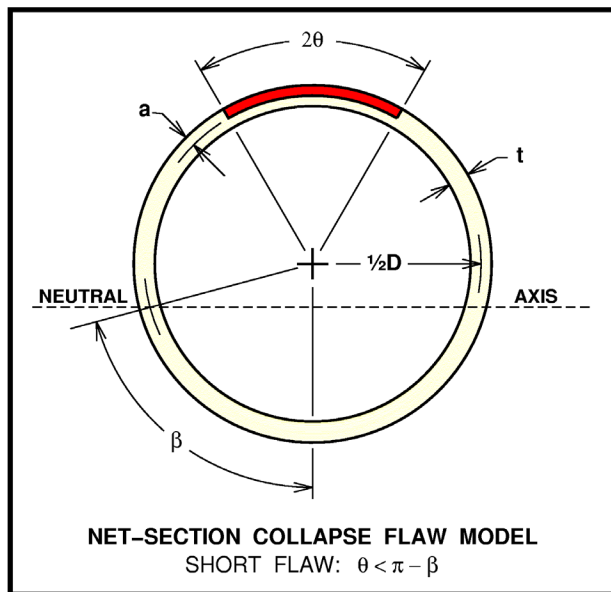
These sketches illustrate the five different types of circumferential flaws in the IPIRG pipe fracture database.

Figure 2: IPIRG Pipe Fracture Database – Flaw Types



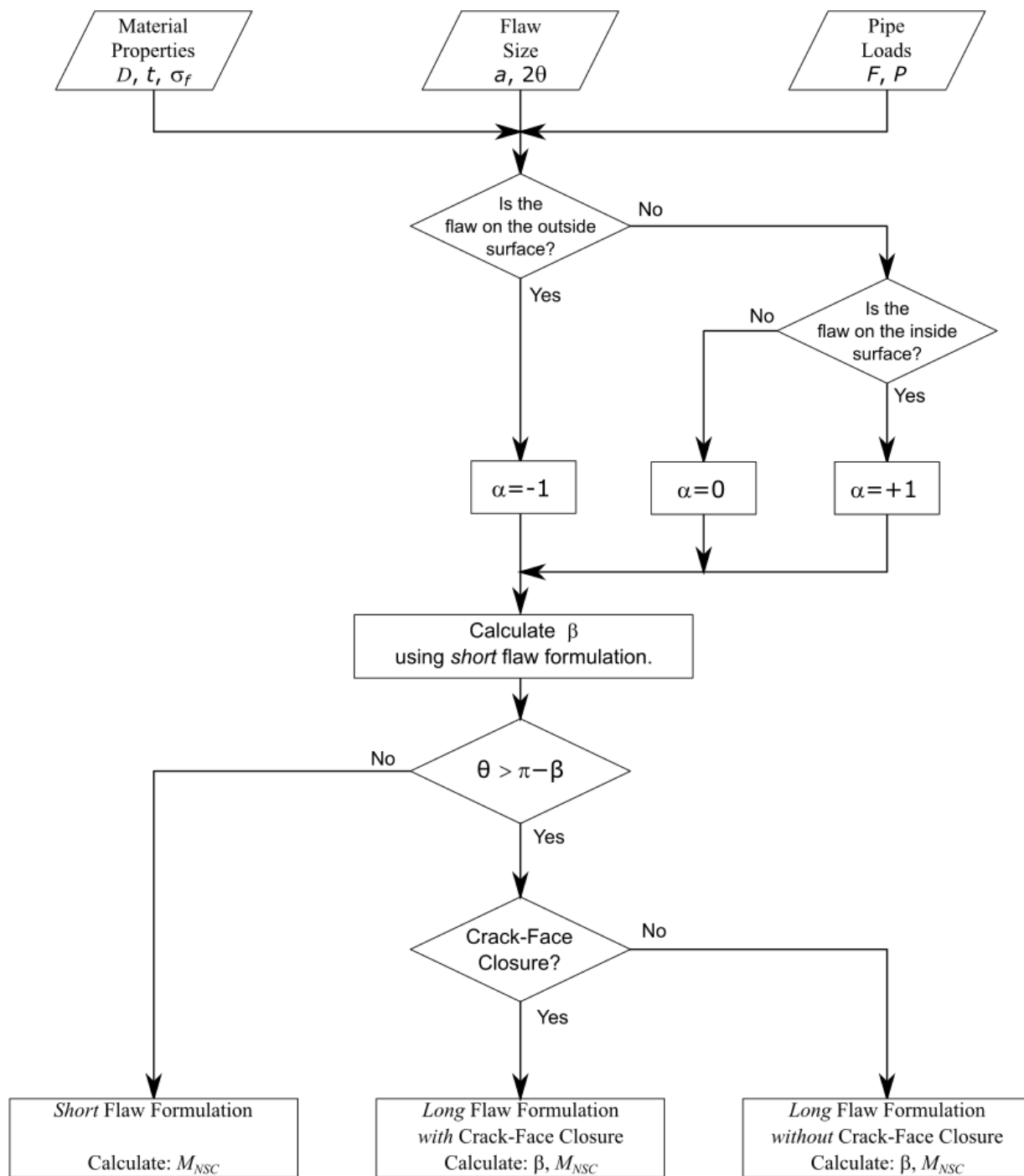
This sketch illustrates the nomenclature for the NSC flow model. The crack is idealized as a constant-depth crack with a depth of a and a circumferential extent of 2θ in a pressurized pipe. The presence of the degraded area results in a shifting of the neutral axis for the cross section below the centre-line of the pipe as determined by the angle β . The material is characterized as rigid perfectly plastic. The axial stresses above the neutral axis are tensile with a magnitude of the flow strength (σ_f) and the axial stresses below the neutral axis are compressive with a magnitude of the flow strength.

Figure 3: Net-Section Collapse Flaw Model



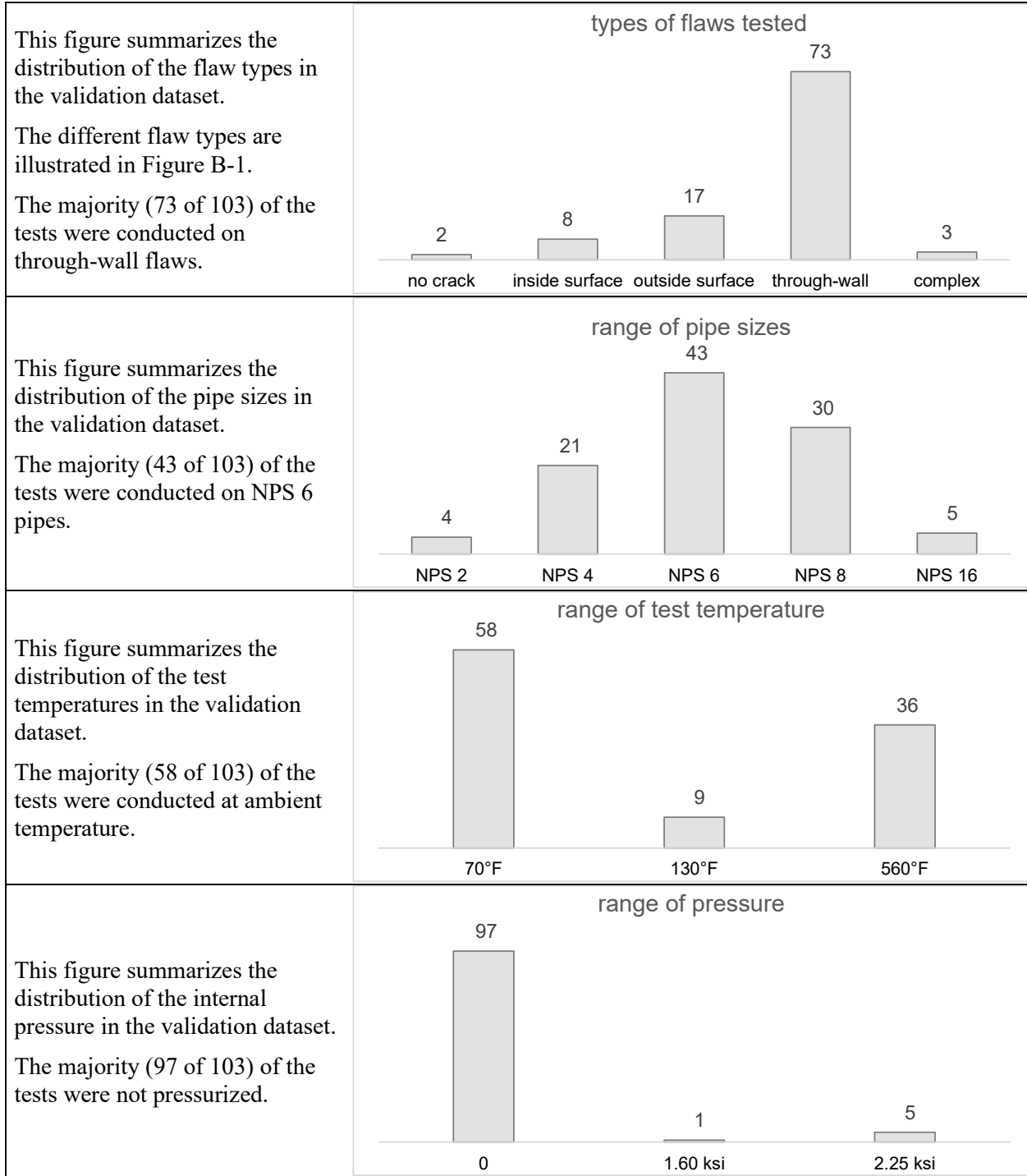
These sketches illustrate the three different flaws that are considered. In the case of long flaws, consideration is given to the case where the faces of the flaw in the compressive part of the stress distribution either close, (i.e., come into contact), or do not close. The former is a reasonable assumption for long, tight flaws such as arise from fatigue and stress corrosion cracking, while the latter is appropriate for long notches.

Figure 4: NSC Flaw Model – Flaw Geometries



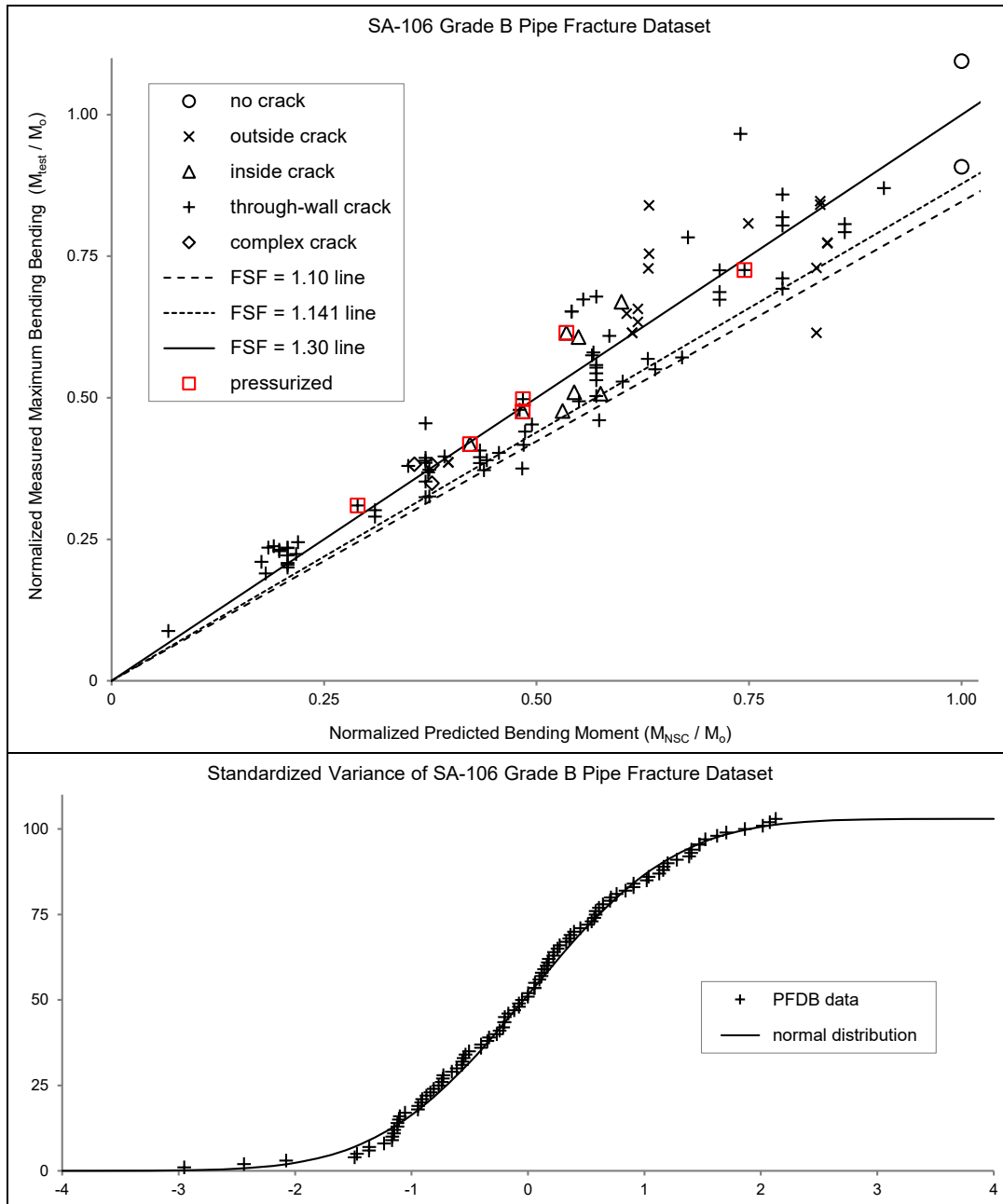
This flowchart illustrates how the net-section collapse flow model is used to calculate the maximum bending moment that can be carried by a section of straight pipe containing a circumferential flaw.

Figure 5: Net-Section Collapse Flowchart



These plots summarize the range of test parameters for the 103 monotonic bending tests in the SA-106 Grade B pipe fracture dataset.

Figure 6: SA-106 Grade B Pipe Fracture Dataset – Test Parameters



The upper figure plots the results of the SA-106 Grade B monotonic bending pipe test dataset versus predicted bending moments using the NSC model. The three lines in the figure correspond to the line where values of M_{test} and M_{NSC} are equal for three different values of the flow-strength factor (FSF):

$$\sigma_f = FSF \left(\frac{S_y + S_u}{2} \right)$$

The lower figure plots the cumulative frequency of the standardized variance for the “best fit” case where the flow-strength factor is $FSF = 1.30$. This validation demonstrates that the net-section collapse flow model is a good engineering model for predicting the maximum load-carrying capacity of pressurized sections of SA-106 Grade B straight pipe containing circumferential flaws.

Figure 7: NSC Model – Validation